Supplementary Information Appendix

Methods

ABBA-BABA (*D* statistics) distribution

To reject the hypothesis that the Tibetan EPAS1-haplotype was from Neanderthals, we calculated the distribution of *D* statistics of the form *D*(Denisovan, Altai Neanderthal, Vindija Neanderthal, Human-Chimp Ancestor) using non-overlapping 32.7-kb windows across the genome (excluding telomeres and centromeres). We chose 32.7kb because this is the length of the haplotype identified in Huerta-Sanchez et al. (2014). We removed archaic sites that had low genotype quality score (<40) and low mapping quality (<30). Within each window, we used two methods of computing the *D* statistic (Durand et al. 2011(1)). First, we randomly sampled an allele from each of the archaic human haplotypes at each side to find sites that matched the ABBA or BABA allele pattern. Second, we used the equation that incorporates allele frequencies to estimate the *D*-statistic for windows with few ABBA and BABA sites. Using this method, we calculated the allele frequency of the derived allele for each individual (1, 0.5, or 0 for 2, 1 or 0 copies of the derived allele respectively) and used those frequencies to make the calculations. The values of *D* statistic obtained across the genome were shown as a density distribution curve in Figure 2b.

Similarly, we computed the value of *D*(Denisovan, Neanderthal, Tibetan, Chimp) at the 32.7kb region in *EPAS1* (chr2:46,567,916:46,600,661, hg19) using the allele frequencies of derived alleles in each population, with Tibetan population being a joined dataset of 78 individuals (40 from Huerta-Sanchez et al. 2014 and 38 from Lu et al. 2016). Using Altai or Vindija individual as Neanderthal yielded the same *D* statistic value, and we show it as a red solid arrow in Figure 2b. We additionally highlight the *D*(Denisovan, Altai Neanderthal, Vindija Neanderthal, Human-Chimp Ancestor) at this window within *EPAS1* as a blue solid line (Figure 2b). We computed the *p*-value of the *D*(Denisovan, Neanderthals, Tibetan, Chimp) at *EPAS1* with Tibetans in the tree using the genome-wide distribution.

Forward Simulations in program SLiM

We used SLiM 3.2.0(2) to perform all simulations in this study. To reduce the computational burden of simulations, we rescaled the simulation parameters in this study by a scaling factor C, where C=10 in this study. The principle of scaling the parameter followed: population size = N/C, times = t/C, selection coefficients = $s \times C$, mutation rate = $\mu \times C$, and recombination rate = $r \times C$. The total length of simulated genomic sequence remained the same. Throughout the paper, we describe the simulation parameters as original parameters before scaling.

We simulated under four different variations of a three-population demographic model described in Figure S7a-d. After a burn-in period of $10\times N$ generations (100,000 generations in this study) of a single population representing the ancestral population of modern and archaic humans. In Model A (results shown in the main text), at 16,000 generations ago, the population split into an archaic population (Denisovans) and the ancestral modern human population. After that, at 2,500 generations ago, ancestral Tibetan population split off from the African population with its population size reduced to 1,860, which describes the Out-of-Africa bottleneck (3). Based on PSMC results for the Tibetans in this study (Lu et al. 2016), the Tibetan population size remained constant until 1,500 generations ago and further reduced to Ne = 1,000. The second bottleneck lasted for 100 generations followed by a population growth into Ne=7000 and remained constant for the rest of the simulation. The end of the second bottleneck is timed so that it is around the European-Asian

split inferred in Ragsdale and Gravel (2019). Subsequently, at a time point drawn from a uniform distribution between 500 generations ago to 2,400 generations ago, a single pulse of gene flow happened from Denisovans into ancestral Tibetans. The admixture proportion was set to 0.1%. Model B shares all demographic parameters with Model A except that the second bottleneck occurred at 920 generations ago with the minimum Ne = 1,160 (4). The end of the second bottleneck is around the time of the European-Asian split time inferred in Gravel et al. 2011. Model C only describes one severe bottleneck effect experienced by ancestral Tibetans, which happened from the Out-of-Africa migrations when the population size reduced to 120 individuals. This bottleneck lasted for 100 generations and then the population recovered to a size of 7,000. Model D differs from Model C by having 1% of admixture proportion.

As for the positive selection on *EPAS1*, we introduced 1 adaptive mutation in the middle of the simulated segment at 15,000 generations ago to all haplotypes in the archaic population to ensure fixation in the archaic population before introgression. The selection coefficient (s) of the adaptive mutation varied between 0 and 0.02 with step size of 0.0002. Right after admixture, the previously adaptive mutation (in the archaic population) was set to be neutral in Tibetans until the specified onset time of selection. For each admixture time, a randomly chosen selection start time was simulated between right after admixture (up to 2,400 generations/72,000 years ago) and as soon as 100 generations ago (3,000 years ago), at average step size of 100 generations. At the time of selection, the selection coefficient of the adaptive mutation in Tibetans resumed to its original value as when introduced in Denisovans, and remained constant until the end of the simulation. We only kept the simulations where the adaptive mutation was not lost in the recipient population by the end of each simulation (adaptive mutation frequency > 0 in Tibetans). We sampled 2, 176, and 156 haplotypes from the Denisovan, African and Tibetan populations respectively, matching the sample size in the empirical dataset of Denisovans, unadmixed Africans (YRI), and Tibetans. We obtained 400,000 replicates under each demographic model for the ABC inference.

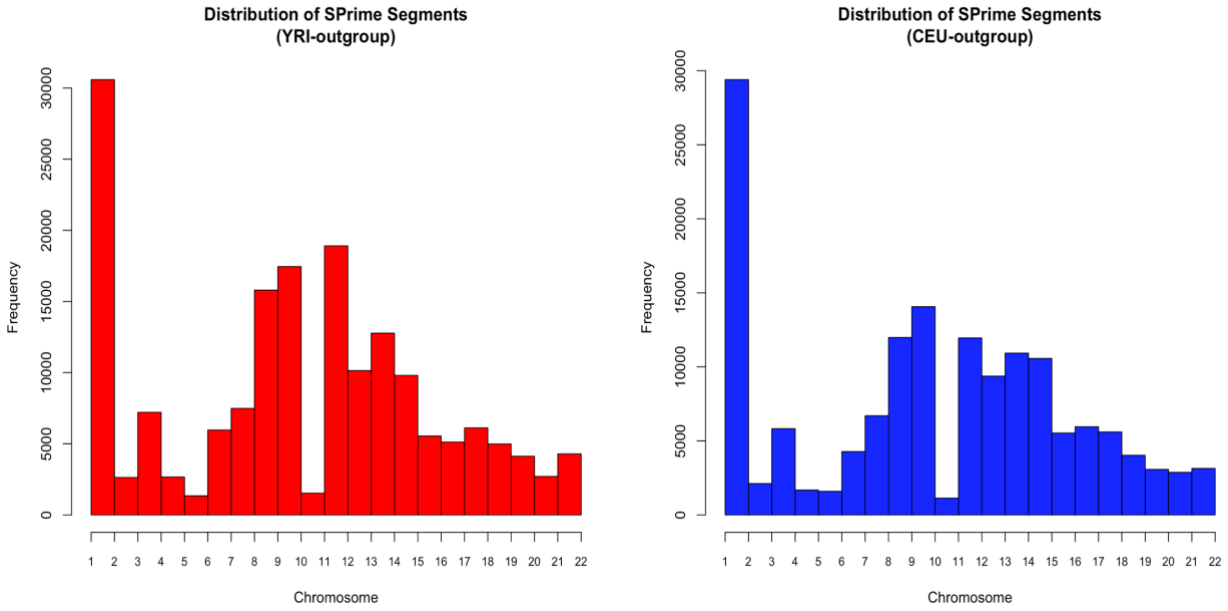

Figure S1: Chromosomal distribution of putatively archaic-introgressed segments inferred using YRI and CEU as outgroup. *This figure shows the distribution of putatively introgressed*

segments on the 22 autosomes, inferred by SPrime using YRI and CEU as outgroup respectively. The X-axis denotes the chromosome number. The Y-axis is the number of segments in the corresponding chromosome.

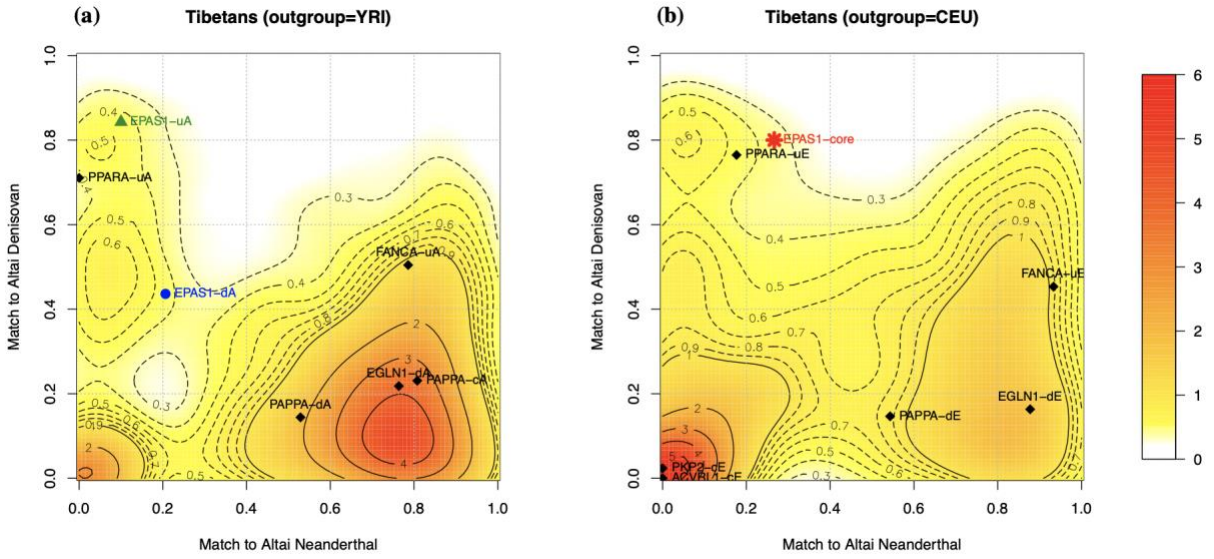

Figure S2: Match rate distribution of introgressed segments in Tibetans. *This figure shows the density distribution of match rate to archaic individuals in putatively archaic introgressed segments in Tibetan population (n=38), inferred by SPrime using Africans as unadmixed outgroup (YRI, panel a) or using Europeans as the outgroup (CEU, panel b). The match rate is defined as the proportion of alleles at the SPrime diagnostic SNPs in a putatively introgressed segment that are present in the genome of archaic individuals at those positions* (5)*. The color range denotes the density of the contours, with red indicating high density and yellow indicating low density. The introgressed segment detected within the EPAS1 gene is highlighted as a star symbol. The introgressed segments detected at or within 200kb range of other high altitude adaptation candidate gene (Table S3) are highlighted as points. After each gene name, "-u/c/d" indicates the location of the segments being in the gene upstream, core, or downstream region respectively. "A" or "E" indicates whether the segment was inferred using Africans (YRI) or Europeans (CEU) as reference.*

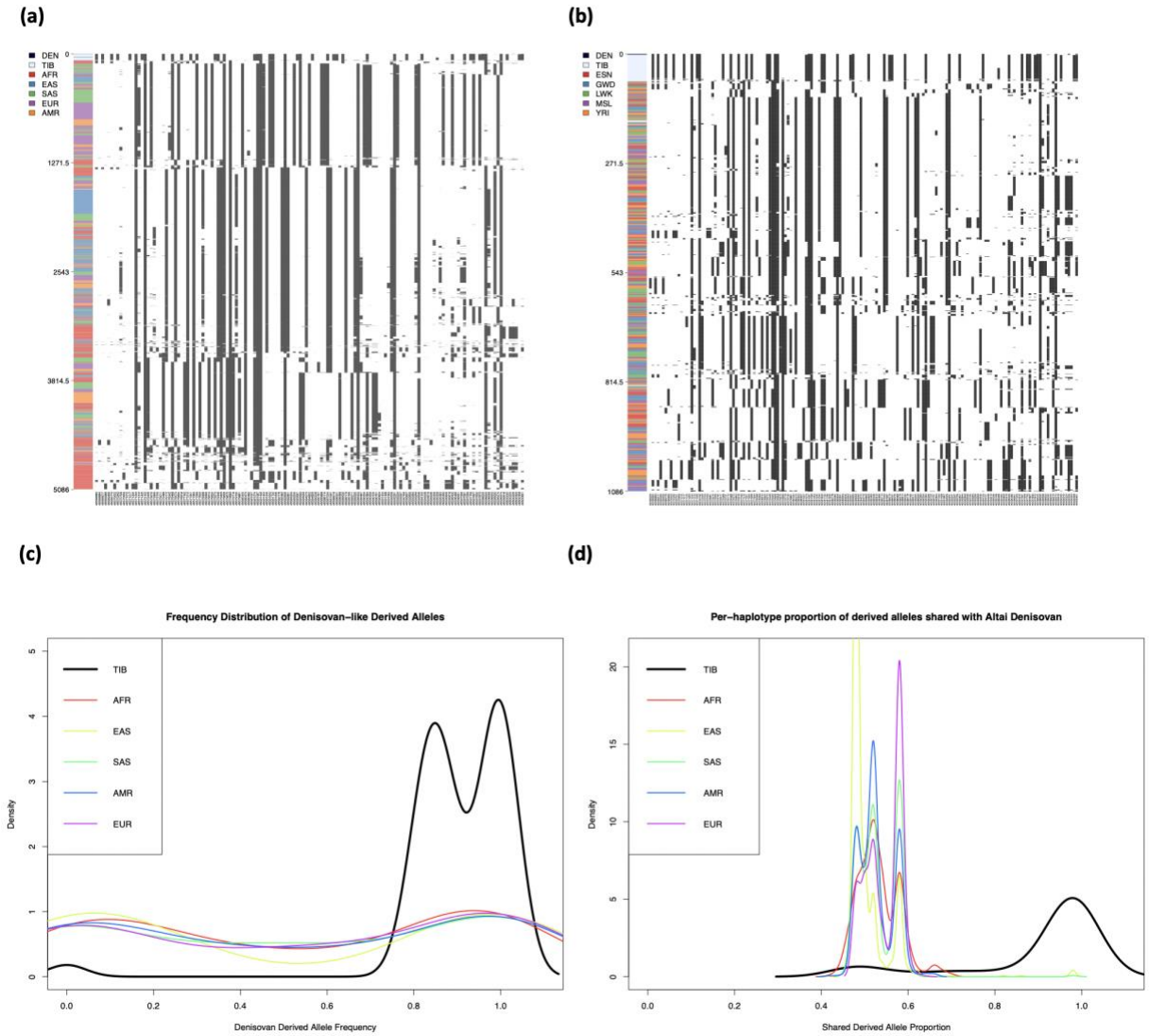

Figure S3. Denisovan-introgressed haplotype at *EPAS1 within the 32.7kb window*. *We show the haplotype patterns of the introgressed segment in the core region of EPAS1 in Denisovan, Tibetans, and worldwide populations (panel a), and Denisovans, Tibetans, and African populations (Panel b) in 1000 Genomes Project using haplostrips program*(6)*. Each column corresponds to a SNP with black cells representing the presence of derived alleles. Each row is a phased haplotype. The colored panel on the left shows the population for haplotypes. Unphased Denisovan genotypes are shown as the top two rows (black). We further plot the frequency distribution of Denisovan-like alleles (defined as the Altai Denisovan carrying the derived allele in homozygous state) within this window in Tibetans and worldwide populations (Panel c), and the distribution of the proportion of Denisovan-like alleles in each haplotype in Tibetans and worldwide populations (Panel d). Altogether, these plots show that although worldwide populations all carry a small amount of Denisovan alleles, only Tibetans carry the alleles in high frequency and in large proportion. The alleles shared between Denisovans and modern humans are unlikely originated from backward gene flow into Africa, but rather, they reflect shared ancestry between Denisovans and modern humans.*

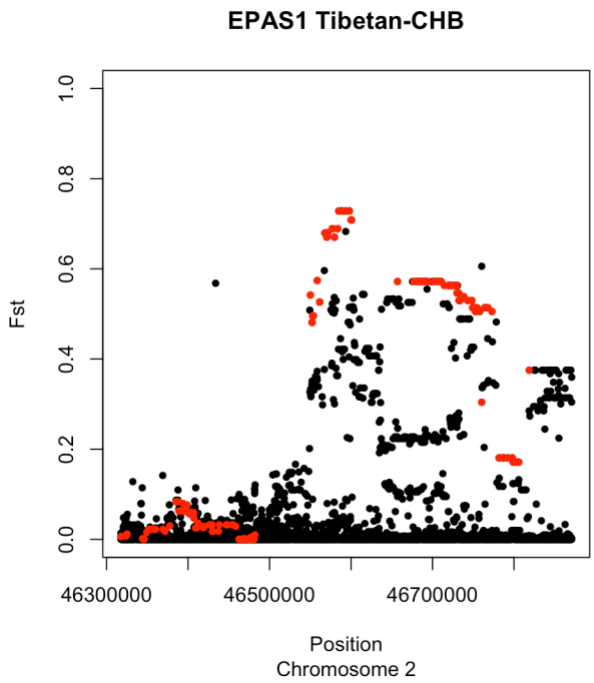

Figure S4: *F_{ST}* between Tibetans and Han Chinese within 200kb of *EPAS1* region. *We show the F_{ST} values of all SNPs at or within 200kb region of EPAS1 in black points. The x-axis shows the genomic position of the SNPs (hg19), and the y-axis shows the F_{ST} value. The red points highlight the diagnostic SNPs that are tagged in this region detected by SPrime (See Table 1). F_{ST} values are calculated between Tibetan and Han Chinese (CHB). The introgressed variants within the EPAS1 region show the highest allele frequency differentiation, indicating positive selection.*

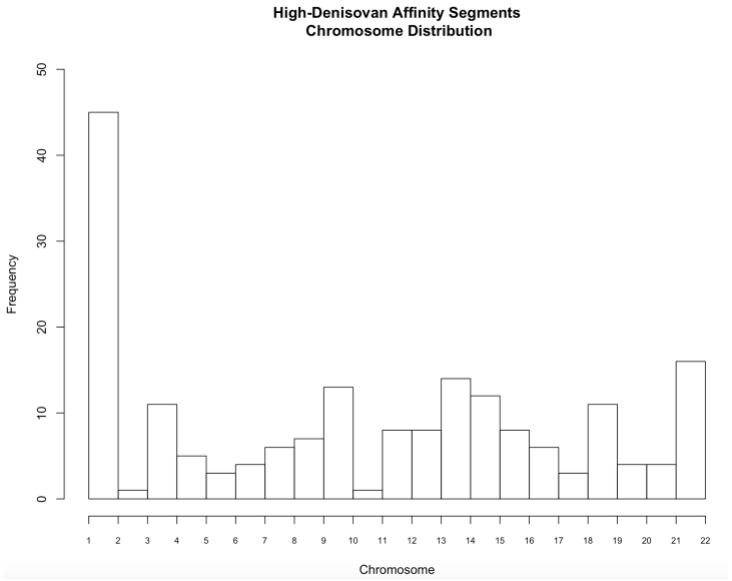

Figure S5. "High Denisovan Affinity" introgressed segment distribution on 22 autosomes. *We show the chromosomal distribution of SPrime segments that have match rate less than 40% to Altai Neanderthal, and larger than 60% to Altai Denisovan, which represent the segments introduced by the East Asian-specific Denisovan introgression.*

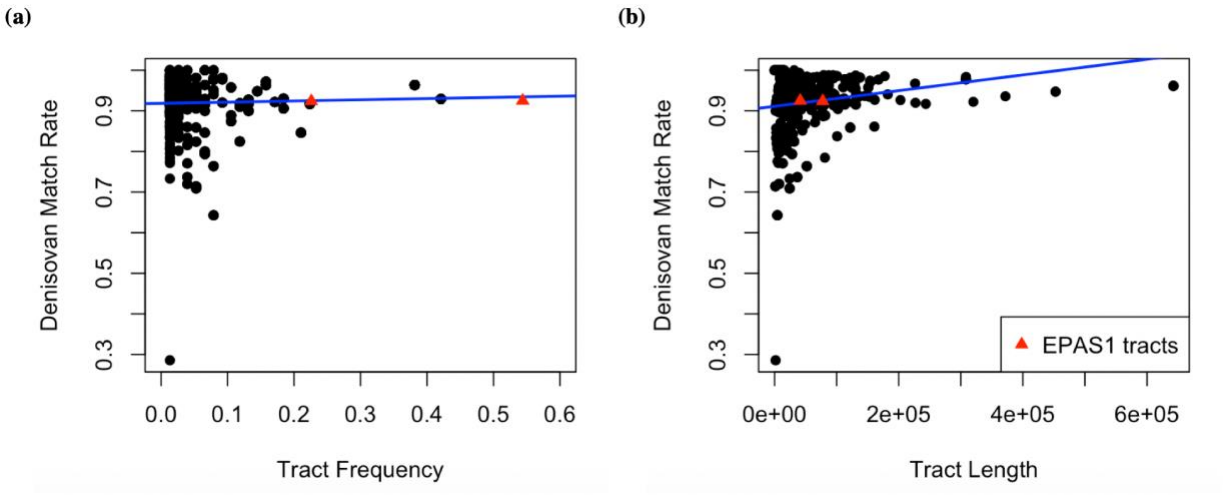

Figure S6. Introgressed tract frequency, length and Denisovan match rate relationship. *This figure shows match rates distribution of Denisovan-introgressed segments, with respect to the frequency of each segment in Tibetan population (panel a), and the length of these tracts (panel b). All segments are detected by HMM from 38 Tibetan whole genomes. The black points represent introgressed tracts inferred by HMM, summarized by tract length. The input genotypes for HMM inference include derived alleles within the range of the first and last diagnostic SNPs in each unique SPrime segment. The red triangle points represent the introgressed tracts at EPAS1, including a long and a short segment (80kb and 40kb respectively, see Figure S9). The tract length is computed by the distance between the first and last position of a continuous introgressed tract inferred from each haplotype. The tract frequency is the number of haplotypes harboring the tract of a specific length divided by the total number of haplotypes. The match rate is defined as the proportion of SNPs in a segment that is present in the Altai Denisovan genome at respective positions.*

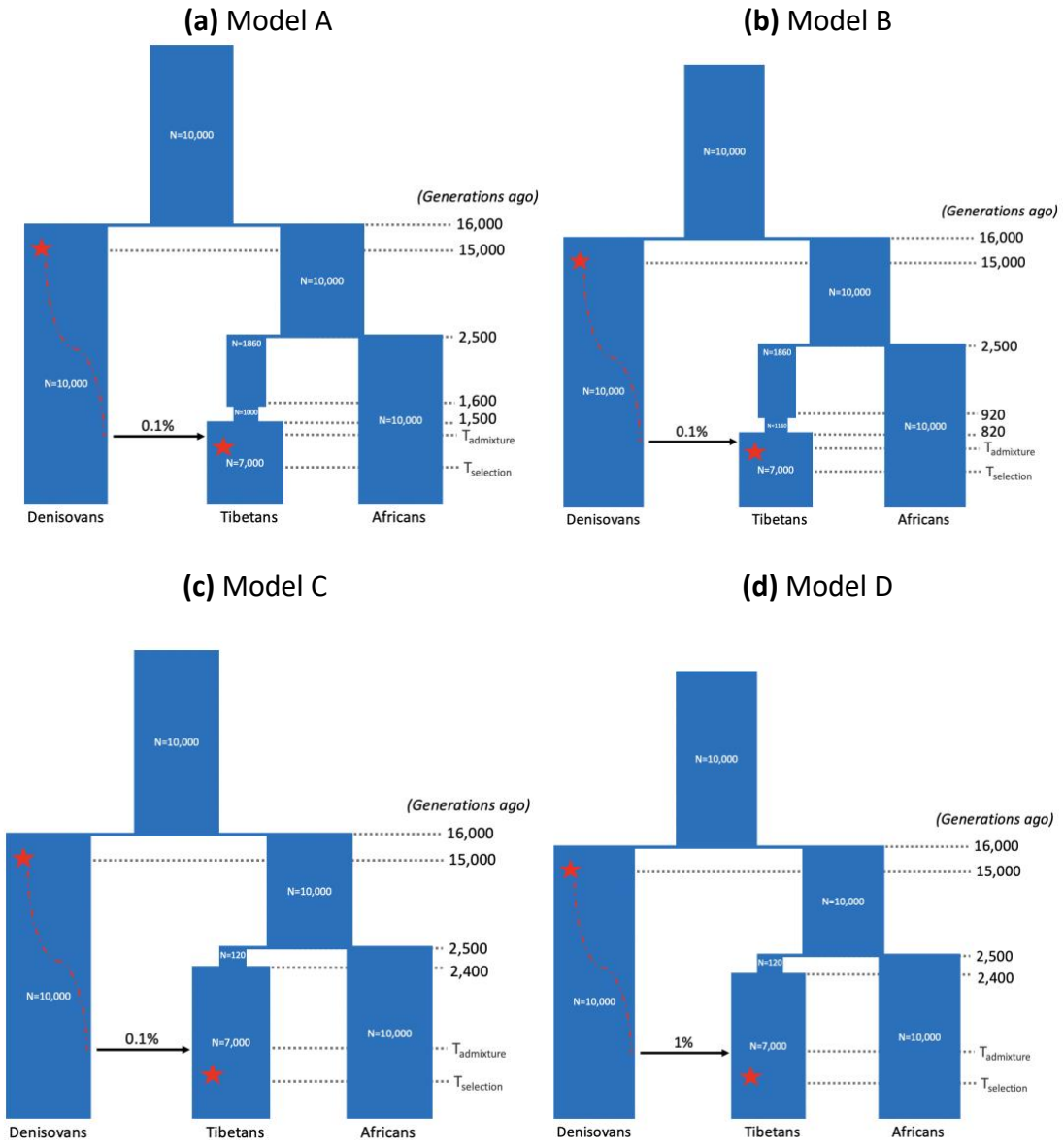

Parameter	Value Range
Admixture time ($T_{admixture}$)	[500, 2400]
Selection start time ($T_{selection}$)	[100, $T_{admixture}$)
Selection Strength	[0, 0.1]

Figure S7: ABC Simulation demography models and parameters. *Panel a-d show four variations of the Denisovan introgression demography simulated for the ABC inference. Model A represents the model used to show results in the main text. These models only vary by the number and duration of bottleneck(s) Tibetans experienced since Out-of-Africa (OoA), and/or the amount of Denisovan introgression. Going forward in time, after a burn-in period of 10*N (100k) generations, the ancestral*

population split into two subpopulations, the archaic (Denisovans) and ancestral modern human populations, at 16k generations ago (g.o). At 15k g.o, an adaptive mutation occurred in Denisovans and became fixed before introgression. The ancestral modern human split into Non-Africans (Tibetans) and Africans at 2.5k g.o. In model A, the population size since the OoA is 1,860, and further shrink to 1,000 at 1.6k g.o. After 100 generations of the second bottleneck, the Tibetan population resumed population size to 7,000, and later received a pulse of introgression such that 0.1% of the ancestry in Tibetans came from Denisovans. Model B is a variation of Model A by having the second bottleneck starting at 920 g.o. with Ne = 1160. In Model C, Tibetans only experienced one strong bottleneck (N = 120) after OoA that lasted for 100 generations, and received 0.1% of Denisovan introgression. Model D is the same with Model C but with 1% of Denisivan introgression. The introgressed EPAS1 mutation had selection coefficient being 0 (neutral) until the onsite time of positive selection in Tibetans. Table S2 has all the parameter estimates for Models A-D.

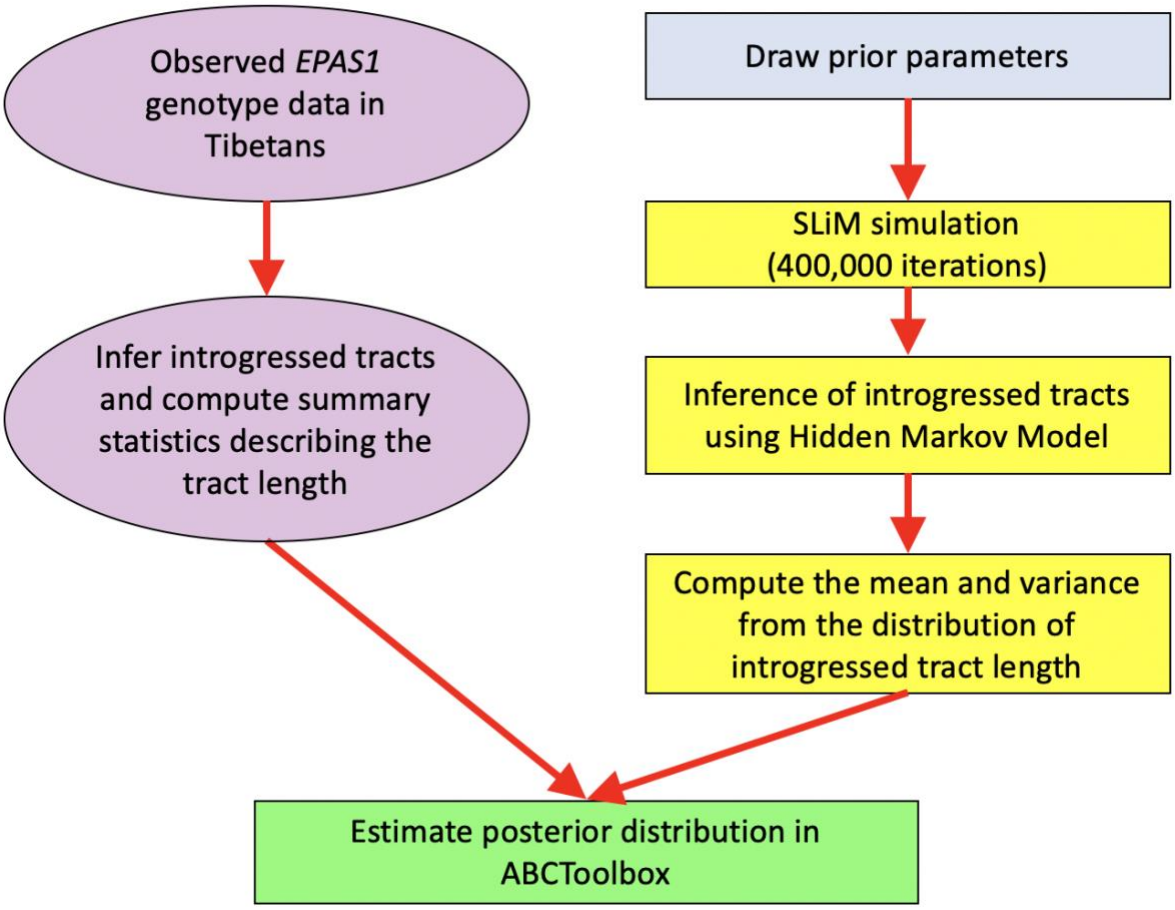

Figure S8: Flowchart illustration of the ABC inference framework

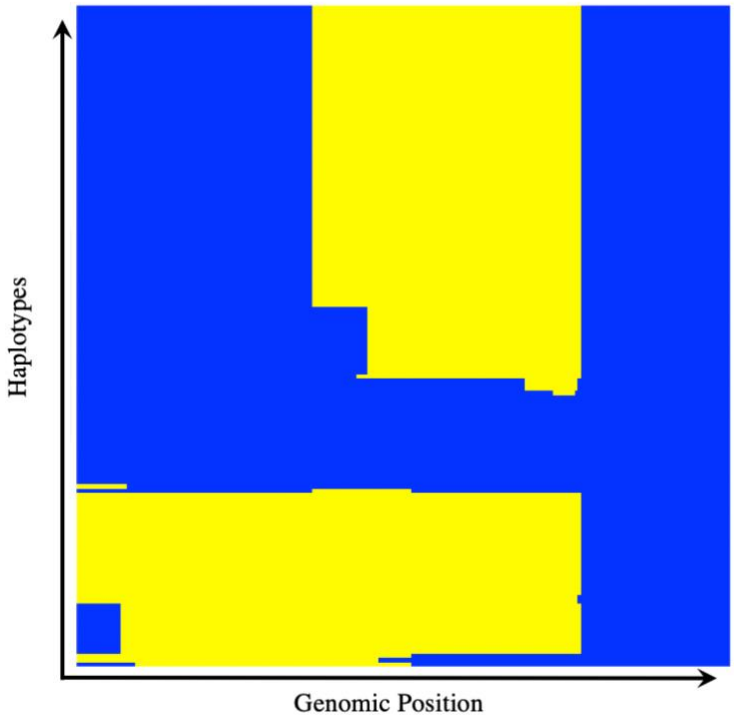

Figure S9: HMM-inferred introgressed tracts in the haplotypes of 78 modern Tibetans at *EPAS1* region. *This figure shows the distribution of introgressed tracts in haplotypes of the combined set of 78 Tibetans at EPAS1, inferred by HMM. The introgressed tracts are highlighted in yellow in respect to the EPAS1 region as blue background. The x-axis shows the genomic position of the tracts, and each horizontal line along the y-axis shows a Tibetan haplotype (156 total).*

(a) Selection on Standing Archaic Variation

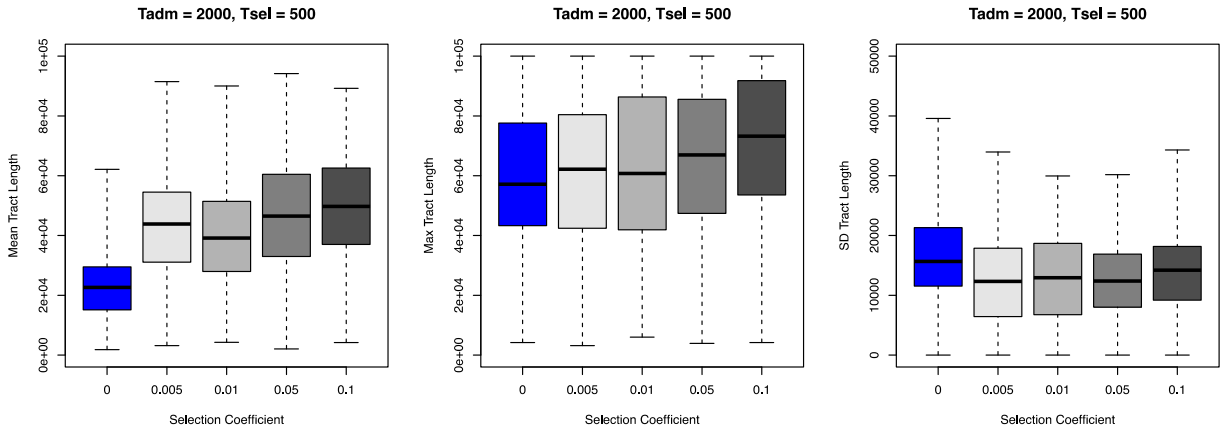

(b) Adaptive Introgression (no neutral period)

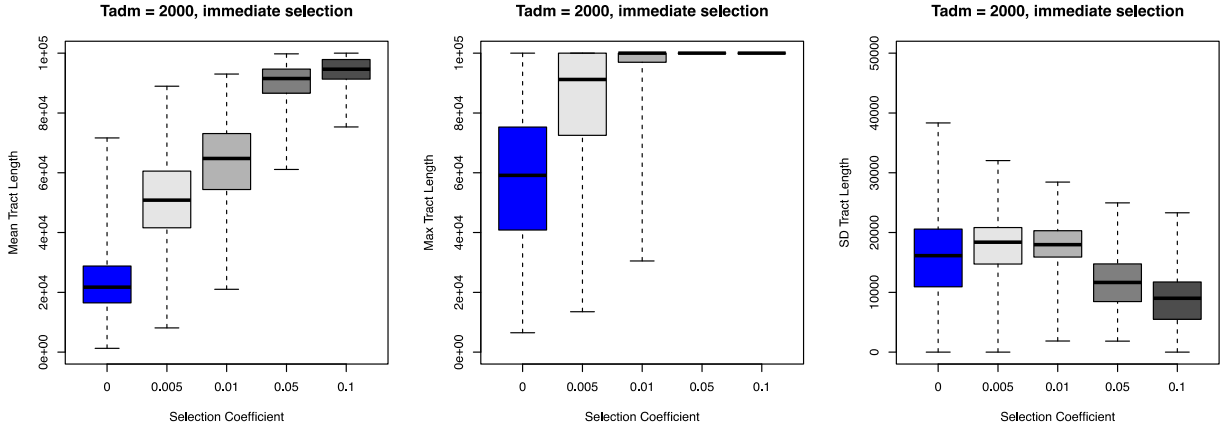

Figure S10: Relationship between introgressed tract length and selection coefficient, admixture time, and selection start time. *We show the relationship between introgressed tract length (summarized by six statistics) and the strength of selection in simulations used for ABC inference. In the simulations, the admixture time (Tadm) is fixed at 2,000 generations ago, and the selection time started either at 500 generations ago (panel a; selection on standing archaic variation), or immediately after the introgression (panel b; adaptive introgression). The introgressed tract lengths are tracked directly from the simulation program SLiM. Each data point in the box plot represents the statistic in all individuals from the admixed population per simulation. Each combination of evolutionary parameters (selection time, selection coefficient) was repeated 5,000 times in simulations. The rest of the demography for the simulations is the same as Model C in Figure S7.*

(a) Model A

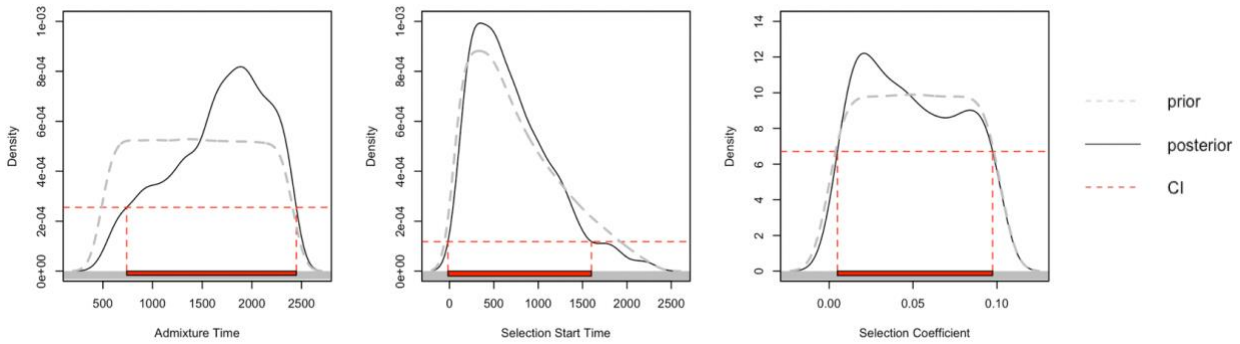

(b) Model B

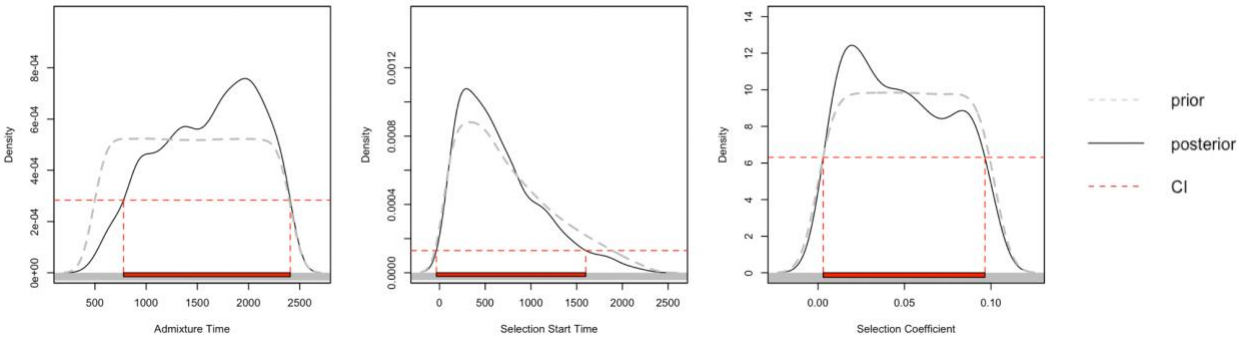

(c) Model C

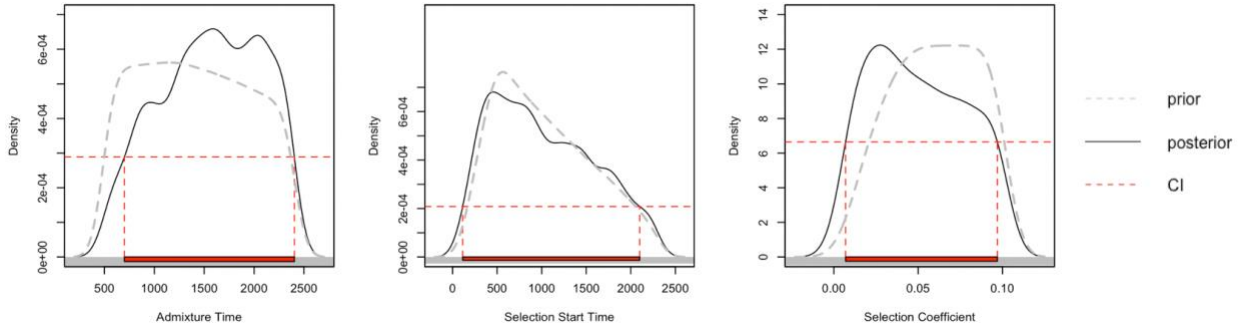

(d) Model D

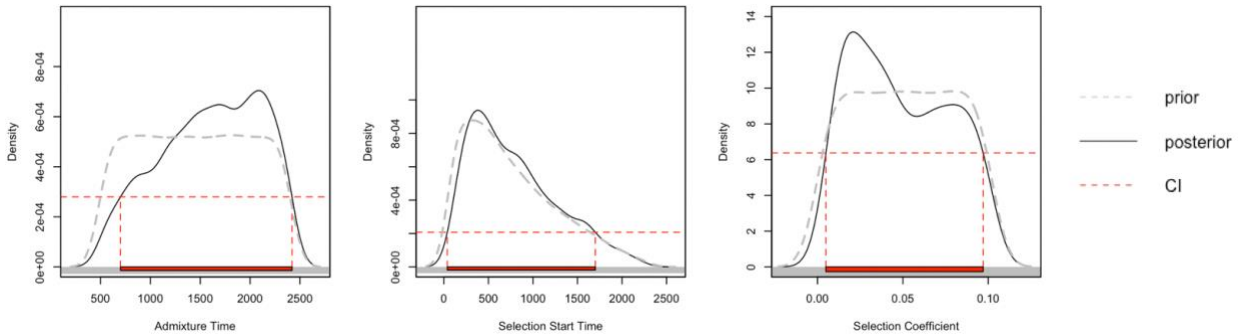

Figure S11: ABC Parameter Estimates. *From panel a-d, the panels show the ABC parameter estimates for the admixture time, selection start time, and selection coefficient, inferred from simulations under the demographic models A-D (Figure S7 and Table S2). In each panel, the gray dotted line shows the density distribution of parameters in the simulations (prior), the black solid line shows the density distribution of 1,000 retained simulations from ABC using rejection algorithm (posterior) from 400,000 simulations, and red dotted line encloses the 95% credible interval range. For the admixture and selection start time, the unit for the values is "generations ago", where one generation is assumed to be 25 years.*

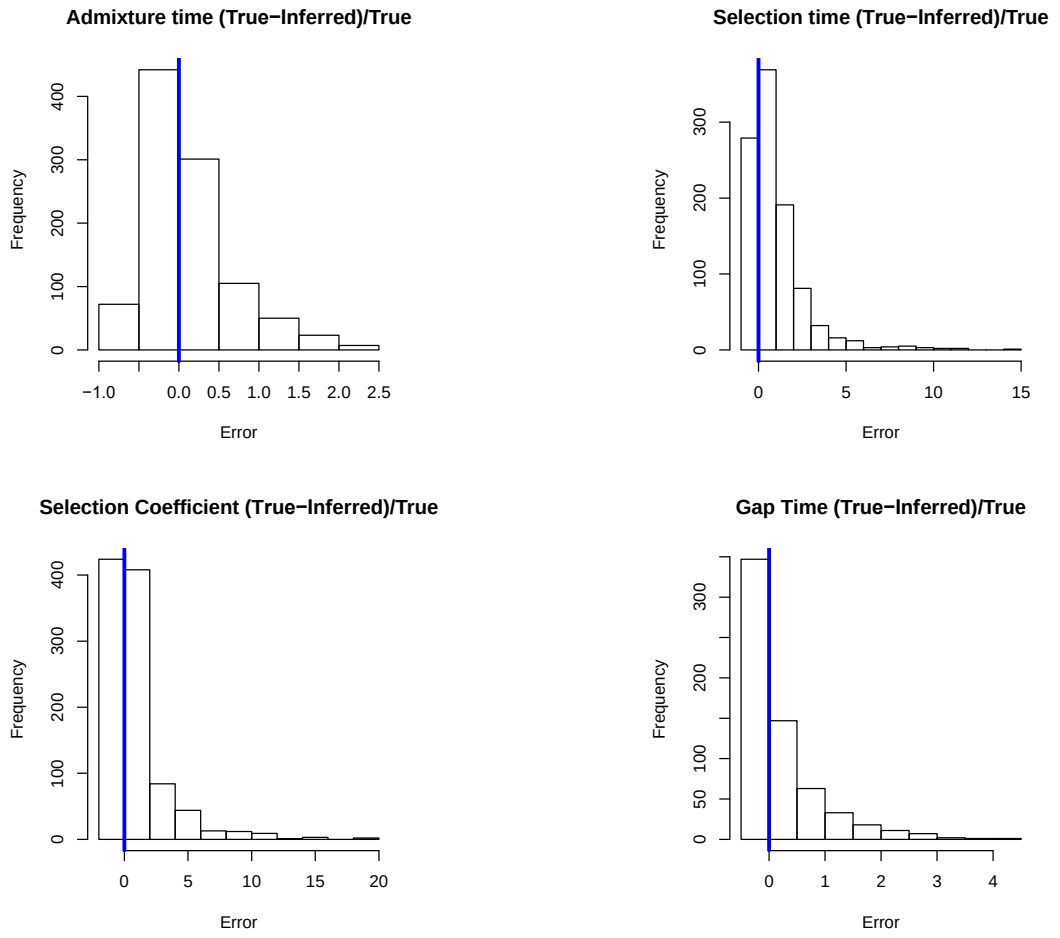

Figure S12: ABC Parameter estimate error distribution from 1,000 randomly chosen simulations under Model A. *In this figure, we vetted the accuracy of the ABC approach by randomly drawing 1,000 simulations from the total of 400,000 simulations (0.1% admixture), and inferred the parameters (admixture time, selection time, selection coefficient) in ABCToolBox using the rest 399,000 simulations. We compared the difference between the inferred parameters and the true parameters in the 1,000 set, and computed "relative errors" (REs) for each summary statistics where RE = (true parameter – inferred parameter)/true parameter. The above figures show the distribution of the errors in admixture time, selection time, selection coefficient, and the difference between admixture and selection time (Gap Time). We show small biases in estimating the parameters, with particularly high accuracy in detecting the gap time between admixture and selection.*

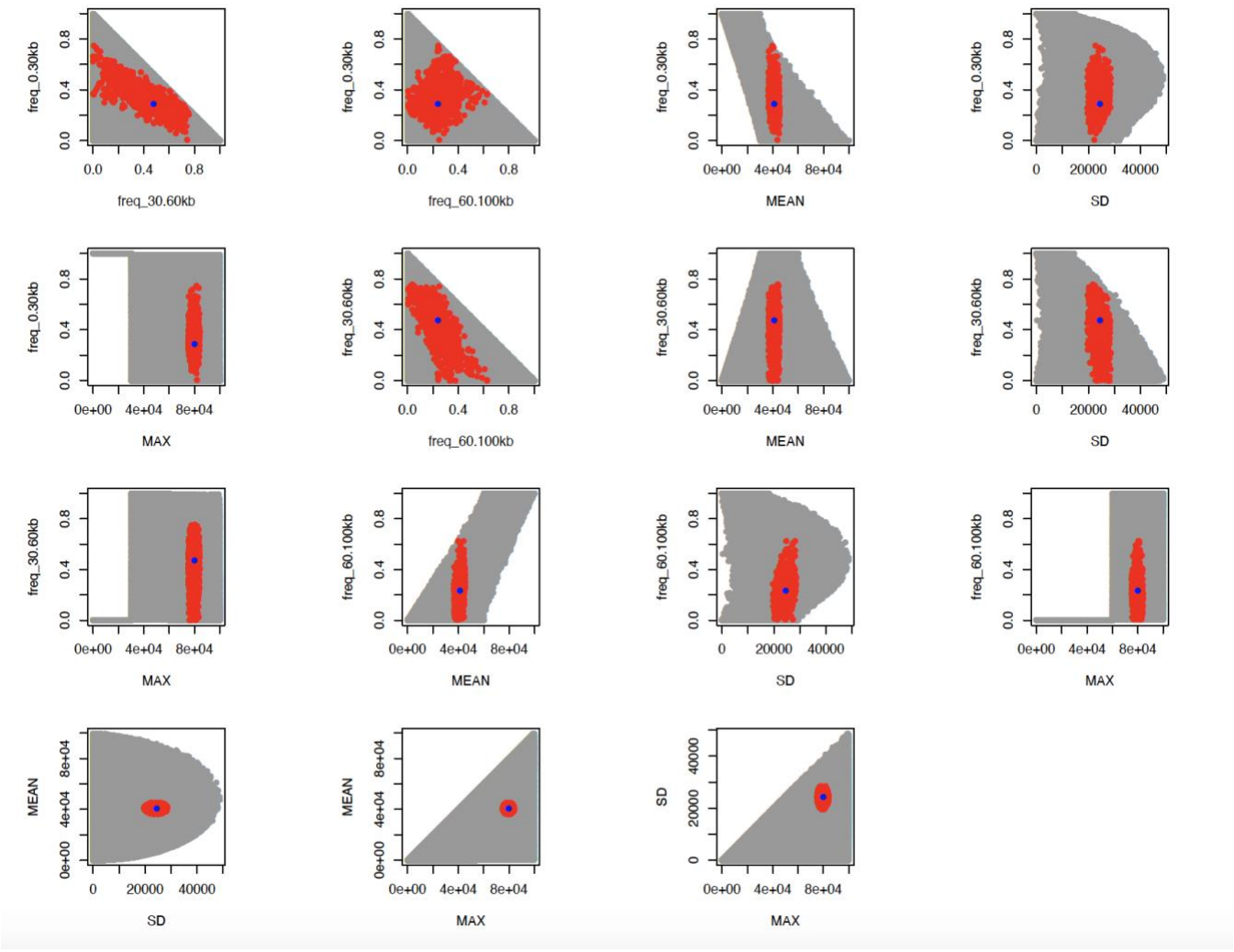

Figure S13: The pairwise distribution of summary statistics used in ABC inference (Model A) from observation, simulations, and retained best simulations. *This figure shows the distribution of pairwise summary statistics between the simulated data under Model A (gray points), retained 1,000 best fitting simulations (red points), and the observed data from 78 Tibetans (blue points). The retained statistics and the observed data show high agreement.*

(a) Summary statistics distribution from retained simulations with sampled parameters

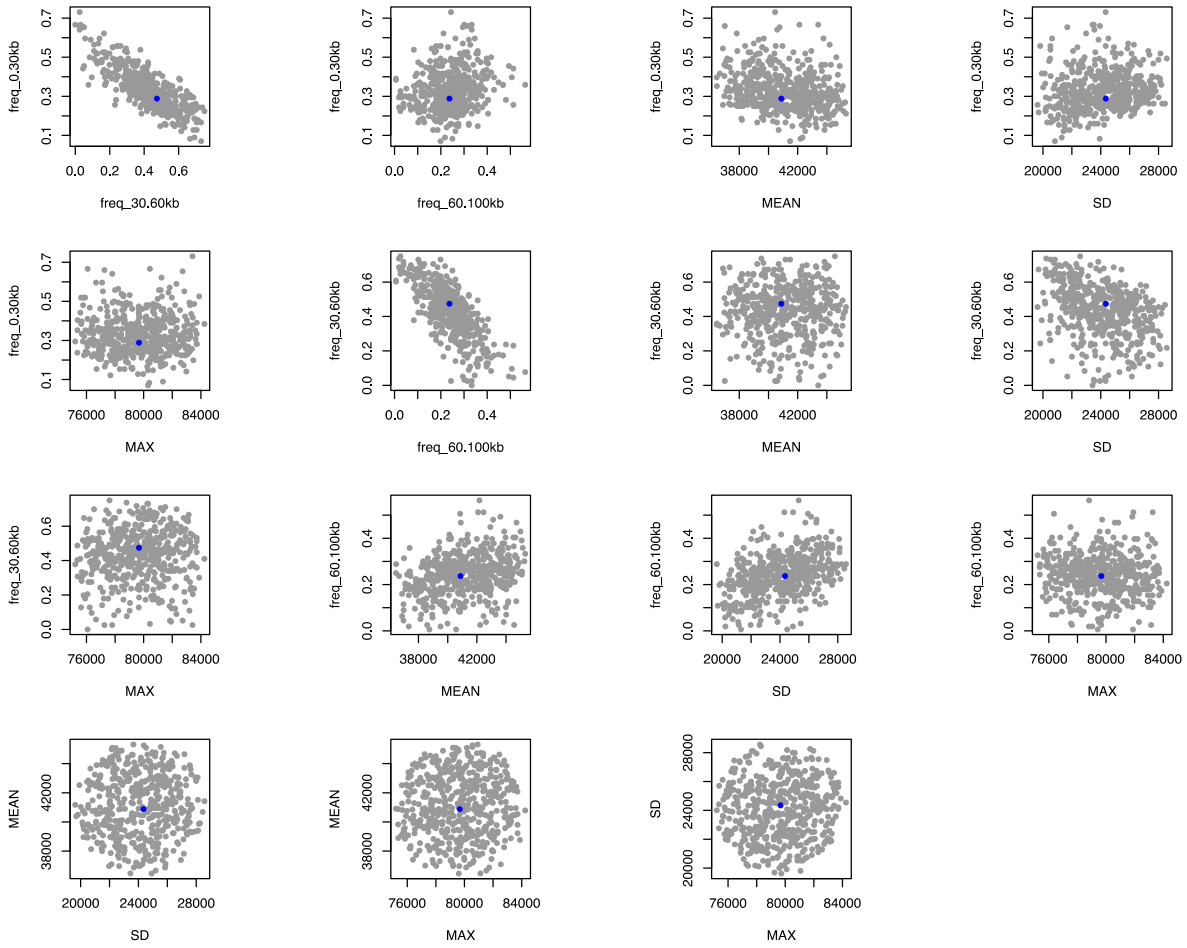

(b) Summary statistics distribution from new simulations using sampled parameters

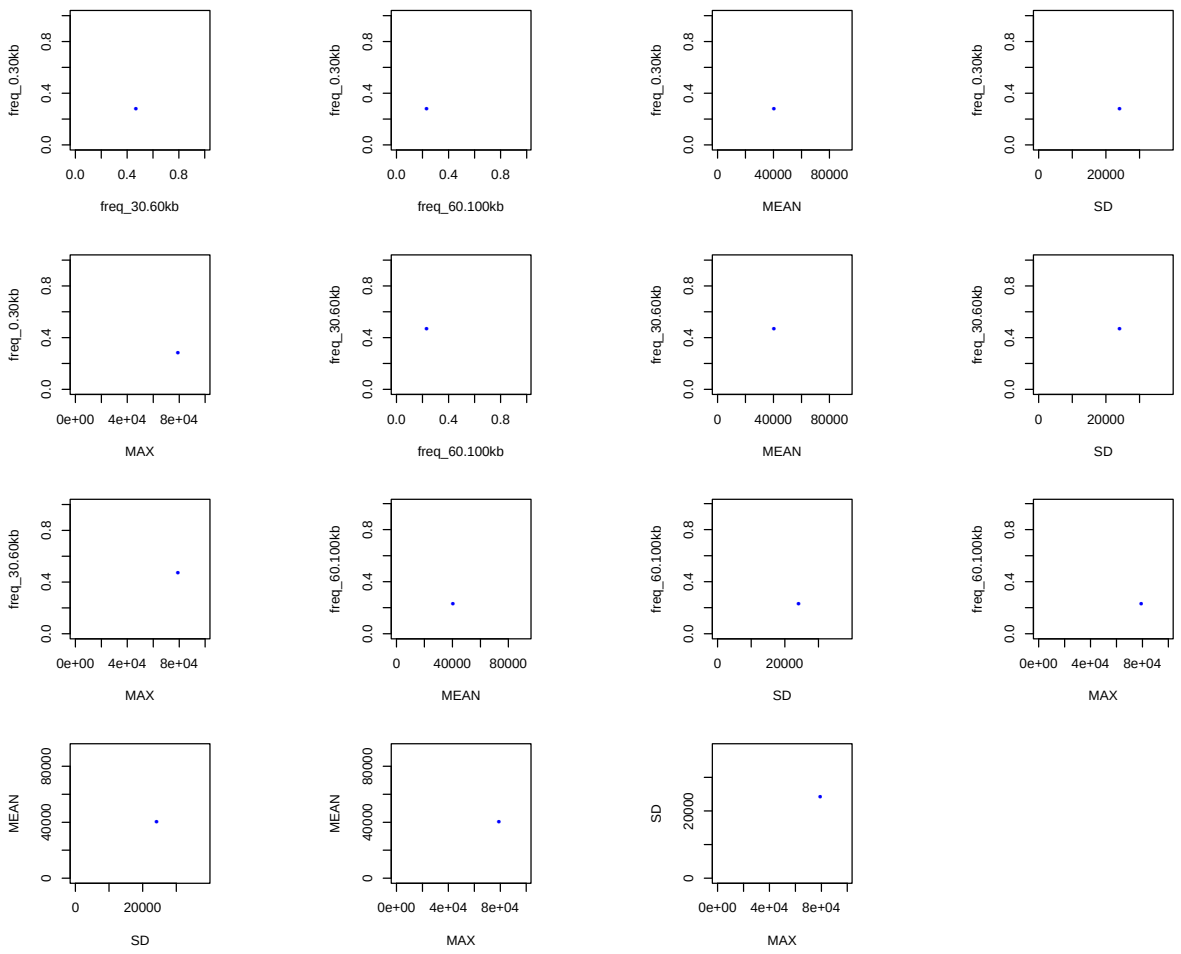

Figure S14: Posterior predictive checking of 500 randomly sampled sets of parameters from retained posterior. *In this figure, we performed posterior predictive checking of the ABC inference by randomly sampling 500 set of simulation parameters from the retained posterior (n=1,000). For each set of parameters, we obtained 1 new simulation using these parameters, and computed the summary statistics in ABC. We compared the original distribution of pairwise summary statistics from the sampled posterior (left panel, posterior in gray points) with regards to the observed data (blue points), and the distribution of pairwise statistics obtained from the new simulations (right panel, new simulations in red points) with regards to the observed data. We show that parameters sampled from the posterior are capable of reproducing the range of summary statistics seen in the posterior.*

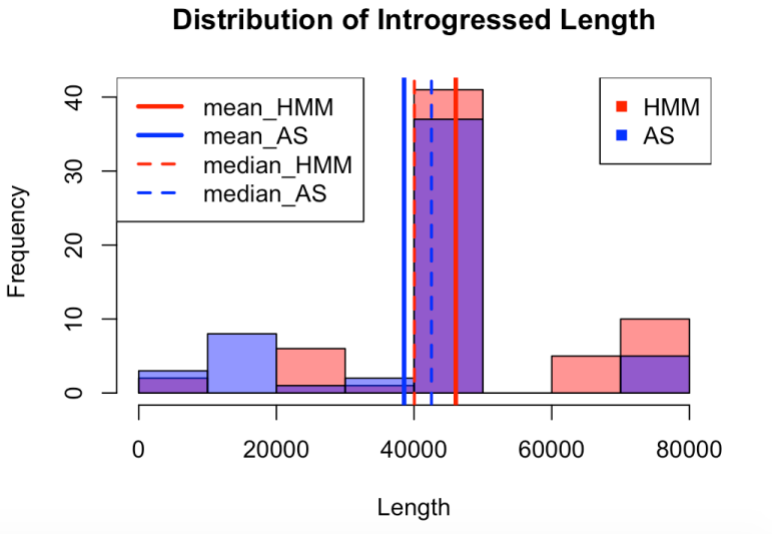

Figure S15: Distribution of introgressed tract length in *EPAS1* region inferred by HMM and ArchaicSeeker 2.0(4)**.** *In this figure, we compared the distribution of introgressed tract length inferred from 38 Tibetans at haplotype level within the EPAS1 region, inferred from HMM (red) and ArchaicSeeker 2.0 ("AS", blue) programs. The solid and dashed lines highlight the mean and median of tract length respectively. We show high level of agreement between the two methods for length inference.*

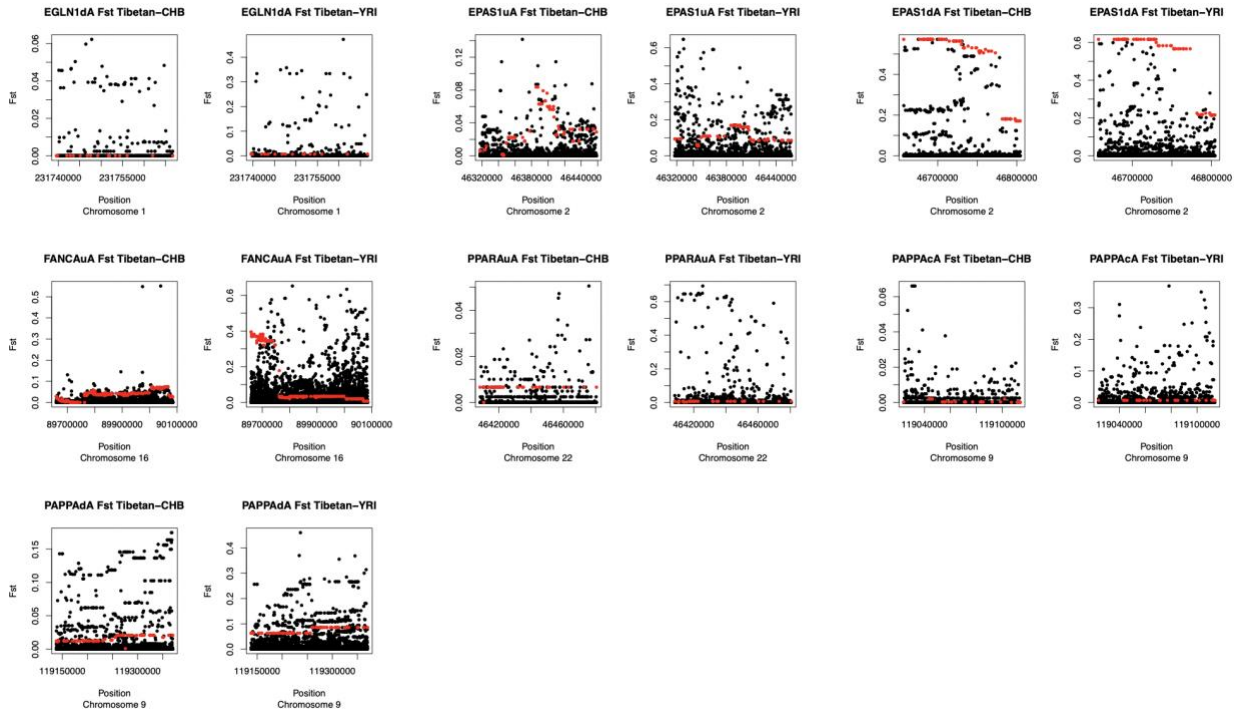

Figure S16: F_{ST} between Tibetans, Han Chinese and Yorubans on segments overlapping between high altitude adaptation candidate genes and SPrime-inferred segments. *The above figure show the F_{ST} values of SNP variants (black points) within SPrime-inferred segments that are at or near high altitude adaptation candidate genes, with introgressed archaic variants highlighted as red points (archaic variants = diagnostic SNPs inferred from SPrime). After each gene name, "u/c/d" indicates the location of the segments being in the gene upstream, core, or downstream region respectively. "A" indicates that these segments were inferred using Africans (YRI) as the outgroup.*

Table S1: Model choice estimates

M1 Marginal Density	M2 Marginal Density	M1 Posterior Probability	M2 Posterior Probability	Bayes Factor M1/M2	Chosen Model
1.41E-19	2.79E-20	0.83	0.17	5.04	1

This table shows the model selection bias between two competing models for the selection of Denisovan EPAS1 allele in Tibetan populations: "Selection on standing archaic variation" model (M1) where a gapped time between introgression and selection is observed, and "Immediate selection on archaic variation" model (M2) where the positive selection is continuous before and after the introgression. We obtained equal number of simulation replicates between the two models (n=400,000), and inferred posterior probabilities using ABCToolBox. The Bayes Factor, which measures the ratio between posterior probabilities of two models, shows a strong favor for M1 over M2.

Table S2: Parameter estimates of *EPAS1* adaptive introgression under demographic models A-D

Parameter	Model A	Model B	Model C	Model D
T_{adm} (generations)	1950.303 (48.76 ka) [639.500 – 2380.000]	1947.424 (48.69 ka) [680.000 – 2360.000]	1741.280 (43.53 ka) [580.000 – 2360.000]	2106.860 (52.67 ka) [580.000 – 2360.000]
T_{sel} (generations)	357.033 (8.93 ka) [100.000 - 1702.500]	301.757 (7.54 ka) [100.000 – 1800.000]	492.055 (12.30 ka) [200.000 - 2200.000]	369.789 (9.24 ka) [100.000 - 1900.000]
Selection coefficient	0.018 [0.005 - 0.099]	0.018 [0.005 - 0.099]	0.018 [0.007 - 0.097]	0.018 [0.007 - 0.099]

This table shows the estimate of the three parameters in ABC inference of the evolutionary history of EPAS1 in Tibetans, including the admixture (T_{adm}), and positive selection start time (T_{sel}), and the selection coefficient. We show the point estimates of parameters using the mode of the posterior distributions, and 95% credible intervals. We convert times to year units by assuming that one generation is 25 years.

Table S3: High Altitude Adaptation-Associated Genes

Chromosome	Start Position (hg19)	End Position (hg19)	Gene Name
1	155034154	155496154	*PKLR*
1	158373495	158863506	*SPTA1*
1	176225306	177018970	*PAPPA2*
1	231292497	231767790	*EGLN1/DISC1*
2	46317540	46820842	*EPAS1*

2	108656650	109211270	*SULT1C3*
2	203896163	204503892	*CYP20A1*
5	58057865	59990925	*PDE4D*
6	25860489	26322489	*HFE*
6	71170478	71778716	*SMAP1*
9	118709070	119371600	*PAPPA*
10	89416194	89935532	*PTEN*
10	104362789	104824789	*CYP17A1*
11	5038034	5500034	*HBB/HBE*
12	32736679	33256780	*PKP2*
12	33321347	33799754	*SYT10*
12	52078173	52540173	*ACVRL1*
12	120220647	120739299	*CCDC64*
15	48192879	48654879	*SLC24A5*
16	4311533	4773533	*HMOX2*
16	89596958	90090065	*FANCA*
22	41281613	41783081	*EP300*
22	46339498	47140067	*PPARA*
X	12763286	13225286	*TMSB4X*

Table S4: Denisovan-like allele frequency distribution in worldwide populations within the 32.7kb window in *EPAS1*

CHROM	POS	REF	ALT	Freq_DEN	Freq_TIB	Freq_AFR	Freq_EAS	Freq_SAS	Freq_EUR	Freq_AMR
2	46568680	A	G	1.000	0.816	0.059	0.008	0.002	0.001	0.006
2	46569017	A	G	1.000	0.816	0.059	0.008	0.002	0.001	0.006
2	46569770	G	A	1.000	0.816	0.070	0.008	0.002	0.001	0.004
2	46570342	G	A	1.000	0.816	0.036	0.009	0.002	0.001	0.004
2	46571017	C	G	1.000	0.816	0.005	0.008	0.002	0.000	0.000
2	46571243	T	C	1.000	1.000	0.835	1.000	1.000	0.999	0.987
2	46571435	G	C	1.000	0.816	0.000	0.008	0.002	0.000	0.000
2	46575388	A	G	1.000	0.829	0.231	0.103	0.289	0.195	0.340
2	46576488	T	C	1.000	0.868	0.490	0.244	0.600	0.714	0.614
2	46576918	T	C	1.000	0.829	0.067	0.010	0.002	0.000	0.003
2	46577251	T	C	1.000	0.829	0.000	0.010	0.002	0.000	0.000
2	46577299	A	G	1.000	0.868	0.125	0.150	0.372	0.501	0.264
2	46579273	A	G	1.000	0.829	0.210	0.102	0.296	0.235	0.367
2	46579348	T	C	1.000	0.961	0.573	0.787	0.411	0.294	0.388
2	46579658	A	G	1.000	1.000	0.818	0.906	0.712	0.784	0.643
2	46581087	T	C	1.000	1.000	0.859	1.000	1.000	1.000	0.991
2	46581643	T	C	1.000	0.868	0.297	0.137	0.359	0.473	0.244
2	46581732	G	C	1.000	0.868	0.296	0.137	0.359	0.472	0.244

2	46583593	A	G	1.000	0.868	0.482	0.240	0.640	0.638	0.588
2	46584859	A	G	1.000	0.855	0.000	0.010	0.002	0.000	0.000
2	46587034	T	G	1.000	0.987	0.708	0.908	0.772	0.871	0.690
2	46589032	C	T	1.000	0.855	0.110	0.010	0.003	0.022	0.017
2	46590384	C	G	1.000	0.895	0.604	0.231	0.583	0.654	0.597
2	46592807	C	T	1.000	0.855	0.123	0.008	0.003	0.022	0.022
2	46594122	A	G	1.000	0.855	0.003	0.008	0.002	0.000	0.000
2	46597581	T	C	1.000	0.895	0.474	0.342	0.499	0.758	0.448
2	46597756	A	C	1.000	0.855	0.002	0.008	0.005	0.046	0.039
2	46597827	A	G	1.000	0.882	0.248	0.222	0.413	0.539	0.267
2	46598025	C	G	1.000	0.855	0.000	0.008	0.002	0.000	0.000
2	46598233	A	G	1.000	0.974	0.889	0.803	0.609	0.512	0.771
2	46599373	A	C	1.000	0.974	0.839	0.813	0.636	0.474	0.732
2	46600226	T	G	1.000	0.000	0.365	0.000	0.003	0.067	0.088
2	46600661	A	C	1.000	0.842	0.107	0.008	0.002	0.000	0.010

This table shows the Denisovan-like allele frequency distribution in Tibetans and 1000 Genomes super-populations (AFR = Africans; EAS = East Asians; EUR = Europeans; SAS = South Asians; AMR = Americans). We define Denisovan-like alleles being the genomic positions where the Altai Denisovan carries the derived allele in homozygous state. We show that Tibetans have high frequencies (>0.8) in the vast majority of the alleles, while the worldwide populations all carry a small proportion of the Denisovan alleles, they are mostly in low frequencies.

Table S5: SPrime-inferred archaic introgressed segments that overlap with sequenced regions of HAA-related genes (YRI as outgroup)

Chromosome	Position Range (Hg19)	Target Gene	Overlapping Genes	Location to the Target Gene	Segment Label	Match Rate with Altai Neanderthal (%)	Match Rate with Altai Denisovan (%)
1	231739562-231873278	EGLN1	***DISC1,*** *LINC00582, TSNAX-DISC1*	Downstream	EGLN1-dA	75.86	24.14
2	46298751-46458516	EPAS1	***PRKCE***	Upstream	EPAS1-uA	13.51	83.78
2	46657114-46808047	EPAS1	***TMEM247, ATP6V1E2, RHOQ,*** *RP11-417F21.1*	Downstream	EPAS1-dA	22.53	46.48
9	119023930-119113818	PAPPA	--	Core	PAPPA-cA	82.14	28.57
9	119137972-119470221	PAPPA	***ASTN2, TRIM32, AL137024.1***	Downstream	PAPPA-dA	48.31	14.41
12	33736191-34854345	SYT10	***ALG10,*** *RP13-359K18.1*	Downstream	SYT10-dA	76.18	4.22
12	52432776-52626674	ACVRL1	***NR4A1, OR7E47P,*** ***ATG101,*** *RP11-1100L3.7,* ***KRT80***	Downstream	ACVRL1-dA	75.81	9.68
16	89659406-90188467	FANCA	***CPNE7, CDK10, DPEP1, CHMP1A, SPATA2L, SPIRE2, MC1R, TCF25, CENPBD1, DBNDD1, SPATA33, AC092143.1,*** *VPS9D1-AS1,* ***ZNF276, DEF8, TUBB3,*** *RP11-566K11.5, AFG3L1P*	Upstream, Core, Downstream	FANCA-cA	76.68	51.21
22	46408289-46480570	PPARA	*CITF22-92A6.1, LINC00899,* ***PRR34,*** *RP6-109B7.5, PRR34-AS1, RP6-109B7.2, RP6-109B7.4, MIRLET7BHG*	Upstream	PPARA-uA	9.09	70.45

The above table shows the Denisovan introgressed segments in Tibetans that overlap with high altitude adaptation (HAA) candidate gene regions (segments inferred by SPrime). Each row represents a unique segment. From left to the right, each column denotes the chromosome of the segment, the genomic coordinate ranges (hg19), the nearby core HAA gene, other overlapped genes (protein-coding genes in bold), the relative location to the nearby HAA gene, the label of the segment (with "-u/c/d" corresponding to upstream, core, and downstream, and "A" corresponding to SPrime outgroup being Yorubans), match rate to Altai Neanderthal, and match rate to Altai Denisovan.

Table S6: Significant high scoring biological pathways ranked by subnetwork score (*p*-value < 0.05)

Pathway	Network size	Subnetwork size	Subnetwork score	*p*-value	Subnetwork genes
p73 transcription factor network	76	5	10.29656462	0.018240343	*BUB3 CLCA2 SIRT1 TP73 WWOX*
TNF receptor signaling pathway	34	3	10.08066121	0.019313305	*MAP2K3 TRADD TXN*
p38 MAPK signaling pathway	22	3	10.08066121	0.019313305	*MAP2K3 MAP3K5 TXN*
Insulin Pathway	42	2	8.891866245	0.0472103	*F2RL2 RHOQ*
Insulin-mediated glucose transport	17	2	8.891866245	0.0472103	*RHOQ VAMP2*

This table shows the biological pathways (NCI database) that are significant (p-value < 0.05) for being enriched with archaic introgressed alleles and are under positive selection in Tibetan population. The archaic alleles used in this analysis include all diagnostic SNPs identified from SPrime. Each row in this table represents a pathway, and each column from left to right represents the pathway's name, the total number of genes included in the pathway (network size), the number of genes involved in positive selection for archaic alleles (subnetwork size), the score assigned from the high scoring subnetwork (HSS) analysis, the p-value of the pathway, and the names of the genes that are under positive selection (subnetwork genes, total number corresponding to the subnetwork size).

Table S7: Time Estimates on Denisovan admixture, Tibetan-Han Chinese Divergence, and *EPAS1* selection from this and other studies.

Date (ka)		Summary Statistics/Methods	Type of Data	Reference
Denisovan Admixture Time in Asia	***EPAS1* Selection Time**			
48.76 [59.50-15.99] **estimate for introgression in East Asia*	8.93 [42.56-2.50]	Distribution of introgressed tract length /ABC	*EPAS1* gene sequence (Tibetans)	This study
45.7 (31.9-60.7) **Shared with Papuans*	-	Distribution of tract length/Maximum likelihood	Whole genome sequence (Papuans)	Jacobs *et al.* 2019(7)

32-12	12.30 (28-7)	Allele frequency, haplotype homozygosity/ Maximum likelihood	Whole genome sequence (Tibetans)	Hu *et al*. 2017(8)
62-38	-	Pairwise nucleotide difference/TMRCA	Whole genome sequence (Tibetans)	Lu *et al*. 2016(4)
44-54	-	Decay of linkage disequilibrium/ Maximum likelihood	Whole genome sequence (Papuans)	Sankararaman *et al*. 2016(9)
-	12.80 (12.07–14.73) **selection not on Denisovan allele*	Extended haplotype homozygosity	Microarray data of *EPAS1* (Tibetans)	Lou at al. 2015(10)
-	18.25 (17.57-18.93)	Extended haplotype homozygosity	Re-sequencing of *EPAS1* (Tibetans)	Peng *et al*. 2010(11)

In this table, 95% confidence intervals (CI) estimated from previous studies are shown in the parentheses. 95% credible intervals estimated from ABC in this study are shown in brackets. Lu et al. 2016 estimated the Time to the Most Recent Common Ancestor (TMRCA) as a proxy of admixture time, assuming the Denisovan and Tibetan lineages coalesce right before the introgression time. Jacobs et al. 2019 inferred 3 pulses of Denisovan admixture in Asia, with one introgressed into the Papuan lineage at 29.8 ka (95% CI 14.4–50.4), and one into the shared lineage of Papuans and other Asians at 45.7 ka (95% CI 31.9–60.7) respectively. That work did not provide an estimate on the East Asian-specific introgression time.

Reference

1. Durand EY, Patterson N, Reich D, Slatkin M (2011) Testing for ancient admixture between closely related populations. *Mol Biol Evol* 28(8):2239–2252.
2. Haller BC, Messer PW (2018) SLiM 3: Forward genetic simulations beyond the Wright–Fisher model. *Mol Biol Evol*:msy228-msy228.
3. Gravel S, et al. (2011) Demographic history and rare allele sharing among human populations. *Proc Natl Acad Sci* 108(29):11983 LP-11988.
4. Lu D, et al. (2016) Ancestral Origins and Genetic History of Tibetan Highlanders. *Am J Hum Genet* 99(3):580–594.
5. Browning SR, Browning BL, Zhou Y, Tucci S, Akey JM (2018) Analysis of Human Sequence Data Reveals Two Pulses of Archaic Denisovan Admixture. *Cell* 173(1):53–61.e9.
6. Marnetto D, Huerta-Sánchez E (2017) Haplostrips: revealing population structure through

haplotype visualization. *Methods Ecol Evol* 8(10):1389–1392.
7. Jacobs GS, et al. (2019) Multiple Deeply Divergent Denisovan Ancestries in Papuans. *Cell* 177(4):1010–1021.
8. Hu H, et al. (2017) Evolutionary history of Tibetans inferred from whole-genome sequencing. *PLOS Genet* 13(4):e1006675.
9. Sankararaman S, Mallick S, Patterson N, Reich D (2016) The Combined Landscape of Denisovan and Neanderthal Ancestry in Present-Day Humans. *Curr Biol* 26(9):1241–1247.
10. Lou H, et al. (2015) A 3.4-kb Copy-Number Deletion near EPAS1 Is Significantly Enriched in High-Altitude Tibetans but Absent from the Denisovan Sequence. *Am J Hum Genet* 97(1):54–66.
11. Peng Y, et al. (2010) Genetic Variations in Tibetan Populations and High-Altitude Adaptation at the Himalayas. *Mol Biol Evol* 28(2):1075–1081.